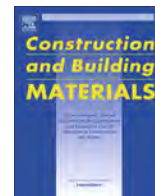




Contents lists available at ScienceDirect

Construction and Building Materials

journal homepage: www.elsevier.com/locate/conbuildmat

Piezoresistive response of conductive Hot Mix Asphalt mixtures modified with carbon nanofibers

Hashim R. Rizvi^a, Mohammad Jamal Khattak^{a,*}, Mohammad Madani^b, Ahmed Khattab^c^a Department of Civil Engineering, University of Louisiana at Lafayette, 254J-Madison Hall, Lafayette, LA 70504, United States^b Department of Electrical Engineering, University of Louisiana at Lafayette, Madison Hall, Lafayette, LA 70504, United States^c Department of Industrial Technology, College of Engineering, University of Louisiana at Lafayette, Lafayette, LA 70504-2972, United States

HIGHLIGHTS

- Dispersing carbon nanofibers in HMA mixtures makes it a smart material with piezoresistive effect.
- Wire embedded electrode provide better results in comparison to plate electrodes.
- Modified HMA mixtures exhibited significant piezoresistivity response at various loading types and temperatures.

ARTICLE INFO

Article history:

Received 31 July 2015

Received in revised form 21 December 2015

Accepted 24 December 2015

Keywords:

Conductive asphalt

Piezoresistivity

Resistivity

Dynamic loading

ABSTRACT

In recent years, “smart structures” experienced significant popularity in civil engineering. Such structures, referred to as *intelligent structures*, are built with combination of smart and conventional materials and have intelligent systems that cannot only gather information and perform tasks, but also sense variation in conditions of the materials and adapt accordingly. Conductive Hot Mix Asphalt (HMA) mixtures are constructed by modifying with electrically conductive materials. Conductive HMA mixtures would potentially make many technologies applicable to pavements including, but not limited to; thermal electric de-icing of airport runways or highways, cathodic protection of concrete bridge decks, pavement damage sensing, truck weigh-in-motion, and so forth. Dispersing carbon nanofibers (CNF) in HMA mixtures makes it a smart material as it develops a piezoresistive effect. The main objective of the study is to develop a smart HMA mixture by using electrically conductive material such as carbon nanofibers (CNF). The CNF modified HMA mixtures would have the ability to respond to loading. An exploratory investigation for piezoresistive response of CNF modified HMA mixtures under various types of loading, frequencies, and temperatures were evaluated. Stress–strain response due to applied load and its relationship with the change in resistivity was discussed. It was found that out of two type of CNF used in the study one provide better piezoresistive response of HMA. It was determined that embedment of copper wire electrodes is the most effective method to achieve smooth and consistent electrical response. Furthermore, polymer modified binders showed promising piezoresistive effect for medium to high temperature range.

© 2015 Elsevier Ltd. All rights reserved.

1. Introduction

In recent years, “smart structures” experienced significant popularity in civil engineering. Such structures, referred to as *intelligent structures*, are built with combination of smart and conventional materials and have intelligent systems that cannot only gather information and perform tasks, but also sense variation

in conditions of the materials and adapt accordingly. High-performance structures, such as skyscrapers, long-span bridges, and dams are the most probable candidates for the application [1] of intelligent structures [1–13].

Conductive Hot Mix Asphalt (HMA) mixtures are constructed by modifying with electrically conductive materials. Commonly used materials for conductive HMA mixtures are graphite, coke, carbon fibers and stainless steel fibers. Conductive HMA mixtures would potentially make many technologies applicable to pavements including, but not limited to; thermal electric de-icing of airport runways or highways, cathodic protection of concrete bridge

* Corresponding author.

E-mail addresses: hrr9588@louisiana.edu (H.R. Rizvi), khattak@louisiana.edu (M.J. Khattak), madani@louisiana.edu (M. Madani), khattab@louisiana.edu (A. Khattab).

decks, pavement damage sensing, truck weigh-in-motion, and so forth [1–19].

Recently, piezoresistive HMA mixture has also been explored by a few researchers. Piezoresistive HMA mixtures were developed by doping the HMA mixtures with conductive materials. Such HMA mixtures would exhibit change in electrical resistivity due to the change in stress or strain response of the material at room temperature. It was found that piezoresistive response would only be optimum in a certain range of compressive stress after which this effect will decrease [20]. It was determined through piezoresistive test results in compressive testing mode, that increase in conductive filler amount was related to piezoresistive response in reverse manner. It was also found that piezoresistive response decreased with the increase in loading cycles. The result of strain to resistivity relationship illustrated that the piezoresistive response of material can be segmented in three parts: initial part of rapid decrease in response, stabilized part of constant response and final part of rapid increase in response. This phenomenon illustrates that change in resistivity of the material decreases initially and then gets stabilized up to an extent where damage starts and this change increases abruptly at the end [20].

Xiao et al. used graphite as conductive filler in HMA mixtures. The mixtures were constructed using 8.5% binder and 5% graphite by weight of aggregates. Wired mesh was embedded in sample to perform two-probe resistivity test. Haversine waveform was utilized under constant stress mode with stress magnitudes ranging from 0.7 to 1.1 Mpa at room temperature. The results of the testing illustrated that effect of piezoresistivity may occur due to three reasons: proximity effect, micro cracks, and dislocation of conductive path due to shear motion of aggregates. It was also concluded that permanent deformation plays an important role in piezoresistive response variations of conductive HMA mixtures [21].

Wu et al. [22] used carbon black, graphite and carbon fiber to design and prepare electrically conductive HMA mixtures. They studied the effects of filler type, filler content and mixed fillers on the resistivity of HMA mixtures. They concluded that the addition of small amounts of expensive carbon fibers to larger amounts of cheaper carbon black or graphite could be a cost effective system. It was observed that the conductive filler particles developed short-range connections whereas the fibers exhibited a long-range conductive bridging effect because of the high aspect ratio [22].

An important consideration while developing a conducting material is resistivity measuring technique. There are two methods available to measure resistivity of the material: one is two-probe and second is four-probe method. Pan et al. showed that two-probe method is functionally applied to the materials showing resistance more than $10^6 \Omega\text{-cm}$ [4]. Wu et al. used two-probe method in order to evaluate the electrical behavior of conductive HMA mixtures. They used steel electrodes with graphite powder to fill in empty spaces on the mixture texture to reduce contact resistance [22]. Two-probe test was not recommended for such testing, as contact resistance could be a potential problem while measuring the resistance. Moreover, wired mesh was also not the right approach to measure the response under loading. Chung found that two-probe method was unreliable due to resistance associated with electrical contacts which would become a part of the final measured resistance [23]. On the other hand four-probe method eliminated the effect of contact resistance thereby providing reliable resistivity readings.

Nano-reinforced materials hold the potential to redefine traditional materials both in terms of performance and potential applications [24–30]. Smart HMA i.e. conductive Hot Mix Asphalt mixture, is a new area of research and requires in-depth study to understand and evaluate interaction of conductive additives with HMA mixture. Dispersing carbon nanofibers (CNF) in HMA mixtures makes it a smart material as it develops a piezoresistive

effect. The electromechanical capabilities of carbon fibers i.e. to sense its own strain due to effect of strain on electrical resistivity can be utilized to develop piezoresistive HMA mixtures. This study has initiated exploratory testing and analysis to evaluate the effective piezoresistive response measuring technique of CNF-modified HMA and the piezoresistive effect at different loading frequencies, temperatures, CNF types and asphalt binder types. This study is a step forward towards the basic understanding of developing smart HMA mixtures using nanofibers.

2. Objective

The main objective of the study is to develop a smart HMA mixture by using electrically conductive material such as carbon nanofibers (CNF). The CNF modified HMA mixtures would have the ability to respond to loading. The specific objectives are:

1. To evaluate and compare different electrode types and embedment techniques to achieve reliable and effective piezoresistive response under dynamic loadings.
2. To evaluate piezoresistive response of HMA mixtures modified with different types of CNF under various loading conditions and at different test temperatures.

2.1. Test materials and sample preparation

2.1.1. Materials

Two types of binders; viscosity graded asphalt AC5 (PG52-22) obtained from a vendor in Atlanta, GA and Polymer modified PAC30 (PG70-28) was used for this research study. PAC 30 and angular limestone were supplied by a local vendor from Abbeville, LA, USA. Two types of Vapor-grown CNF PR-24XT-XTPS and CNF PR-24XT-LHT (Polygraf III) produced by Applied Sciences were utilized for HMA modification. Both CNF has a diameter of 60–150 nm, length of 30–100 μm , average tensile modulus of 600 GPa and average tensile strength of 7 GPa. The CNF has an Iron and Polyaromatic Hydrocarbons content of <1400 ppm and <1 mg PAH/g, respectively. The fiber has a high performance per cost ratio and good interfacial bonding with materials. Thin copper wires of gauge size 12 having diameter of 2.05 mm and thin 0.5 mm copper plates were utilized as electrodes.

2.1.2. Mixing of CNF

It was utmost important to develop a feasible, applicable and time conserving mixing technique in order to blend CNFs in asphalt binder. Authors have published extensive research on mixing techniques and possible solutions to the potential problems related to mixing of CNF and asphalt binder [28,29]. Brief descriptions of the two procedures that were used in the study are as below.

2.1.2.1. Wet mixing process. Partial amount of CNF (usually 1.5% by weight of binder) was homogeneously dispersed in cut back solvent by sonication and high shear mixing. The CNF-solvent mixtures were then mixed with asphalt binder at mixing temperature of 150 °C for AC5 and 175 °C for PAC30 using the shear mixer until all the solvent had evaporated. Remaining amount of CNF (depending on the total dosage to be mixed with HMA) was homogeneously dispersed in solvent using by sonication and high shear mixing. The solvent was allowed to evaporate at room temperature followed by oven heating to obtain fully dried and dispersed CNF. Finally, all required amounts of HMA components including aggregates, CNF modified asphalt binder, and oven dried CNF was heated in an oven at the mixing temperature. All the components were mixed thoroughly using the bench mixer. Homogeneous dispersion

of CNF was achieved using rigorously developed mixing process. Details of mixing procedure can be found elsewhere [27–30].

2.1.2.2. Dry mixing process. This mixing procedure was similar to the above procedure except that dry CNF as obtained from the manufacturer was added in the asphalt binder first and then in HMA mixtures. Small dosage of dry CNF, about 0.3% by weight of binder, was mixed in asphalt using shear mixture at 135 °C. Finally, all required amounts of HMA components including CNF modified asphalt binder, aggregates mixed with remaining amount of CNF were heated in an oven at the mixing temperature. The HMA mixture was thoroughly mixed using the bench mixer.

2.2. HMA mixture design and sample preparation

Superpave mixture design procedure was adopted to conduct the mixture design. The mix design yielded 5.7% optimum asphalt content. The aggregate gradation used for HMA mixture is shown in Table 1.

Piezoresistive response of CNF modified HMA mixtures under various types of compression loading were determined using 150 mm tall and 100 mm diameter cylindrical samples, Fig. 1. The loose HMA mixture heated at compaction temperature was poured in a steel mold in five layers. Each layer consisted of 540 gm of loose HMA mix followed by 5 gyrations of compaction before electrode placement. After all the four electrodes were embedded the sample was placed back in the oven at mixing temperature for 45 min. Finally, 185 gyrations were applied to obtain a fully compacted sample ready for piezoelectric testing under compression loading. The above procedure yielded uniform distance, about 30 ± 2 mm, between the electrode and air void content of $4 \pm 0.5\%$.

2.3. Testing program

2.3.1. Electrical parameter testing

Keithley 225 current source meter was used for constant current supply, Keithley 6487 Picometer/voltage source was used as Amp-meter and Hewlett Packard 34401 multimeter was utilized to determine the voltage output. Voltage response was directly measured by the material testing system (MTS) data acquisition system. Copper wires and copper plates were embedded in the HMA samples as electrodes. The resistivity (ρ , Ω -m) and resistance (R , Ω) were determined using the following sets of equations.

$$\rho = 2\pi sR \quad (1)$$

$$R = \frac{V}{I} \quad (2)$$

where,

ρ = Resistivity of the sample in Ω -m

s = Distance between the electrodes, meters

R = Resistance of the sample between two outer electrodes, Ω

V = Voltage measured between two inner electrodes, Volts

I = Constant current, Amp.

The following parameters were calculated to evaluate the piezoresistive response of the HMA mixtures.

Table 1
Aggregate gradation used for the study.

| Sieve (mm) | 12.5 | 9.5 | No. 4 | No. 8 | No. 16 | No. 30 | No. 50 | No. 100 | No. 200 |
|-------------|------|-----|-------|-------|--------|--------|--------|---------|---------|
| Passing (%) | 100 | 95 | 60 | 42 | 28 | 18 | 11 | 5 | 2 |

$$\% \text{ Change in Resistivity } (\Delta\rho) = \left| \left(\frac{\rho_0 - \rho}{\rho_0} \right) \right| \times 100 \quad (3)$$

$$\% \text{ Change in Resistance } (\Delta R) = \left| \left(\frac{R_0 - R}{R_0} \right) \right| \times 100 \quad (4)$$

$$\% \text{ Change in Voltage } (\Delta V) = \left| \left(\frac{V_0 - V}{V_0} \right) \right| \times 100 \quad (5)$$

where, $\Delta\rho$, ΔR and ΔV are percentage change in resistivity, resistance and voltage due to applied loads, respectively and ρ_0 , R_0 , and V_0 are initial resistivity, resistance and voltage values just before the application of load, respectively.

Fig. 2(a–c) shows typical behaviors of the above three piezoresistive response parameters under sinusoidal loading at frequency of 25 Hz. It can be observed from the figure that all the response parameters follow the same trend and are merely different ways to represent the data. Therefore any of these three parameters could be selected to evaluate the piezoresistive effect of materials. Fig. 2(a–c) shows that piezoresistive response of samples follows the loading cycles in direct manner. This means that the percentage change in V , R , ρ increases or decreases with increase or decrease in applied stress, respectively. On the other hand, the Fig. 2(d) shows that ρ follows the stress signal in reverse manner. This is mainly because of the proximity effect of the electrodes. As the stress level increases the electrodes come closer to each other and hence the ρ of mixture decreases. This trend was observed in all the samples tested in this study.

2.3.2. Electrode embedment

Four-probe method with improvisation was utilized in this study to measure response of CNF modified HMA mixtures. Various researchers have used different types of electrodes to measure electrical parameters such as: steel [24] and copper [16]. These electrodes were fixed on the surface of the sample either at one point or around the whole surface [16,11]. Some researchers used wired-mesh fully embedded in the sample [25]. In this study, the electrodes were embedded in the samples instead of pasting it on the surface to achieve a better contact. An important fact that must be considered is the dependability of the electrical response of the sample on overall electromechanical behavior of CNF. CNF are dispersed in the whole mixture, therefore measuring the response only at the surface of the sample does not seem to be functional. Preliminary results indicated that the resistance of the mixture was very high using surface mounted electrodes. Also, electrical properties can vary significantly with humidity variation in environment. Such variation could be minimized due to embedded electrodes with strong contacts within the mixtures. Results of this study showed that excellent response was acquired during loading, which is significantly low in signal to noise ratio as compare to the previous studies [25].

Two methods to embed the electrode in the HMA sample were investigated: one was after compaction and second was during compaction. Embedding electrodes in compacted sample was difficult and cumbersome whereas it was relatively easy to embed the electrodes during compaction. The effort made to embed the electrodes in compacted sample was not successful. It was determined that copper wire or nails can be embedded in compacted sample either by hammering or drilling. This study explored these techniques and images of the samples with embedded electrodes using hammering and drilling after compaction are shown in Fig. 3(a and b).

Both methods were considered inadequate, as it caused peeling phenomenon. The conductive asphalt binder was peeled off the aggregate hence exposing the uncoated aggregates. Aggregates are insulator in nature therefore the weak contact between

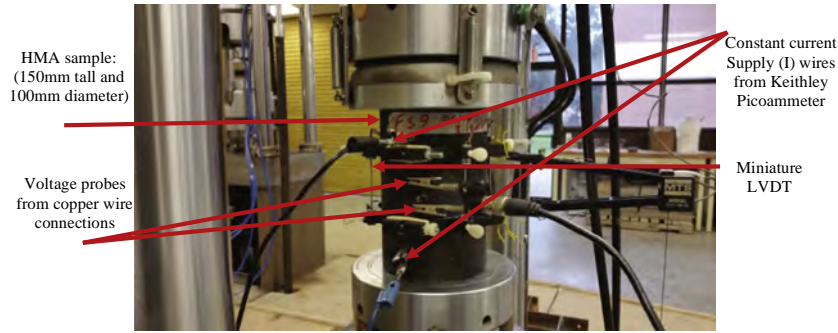


Fig. 1. HMA sample with four embedded thin copper wires.

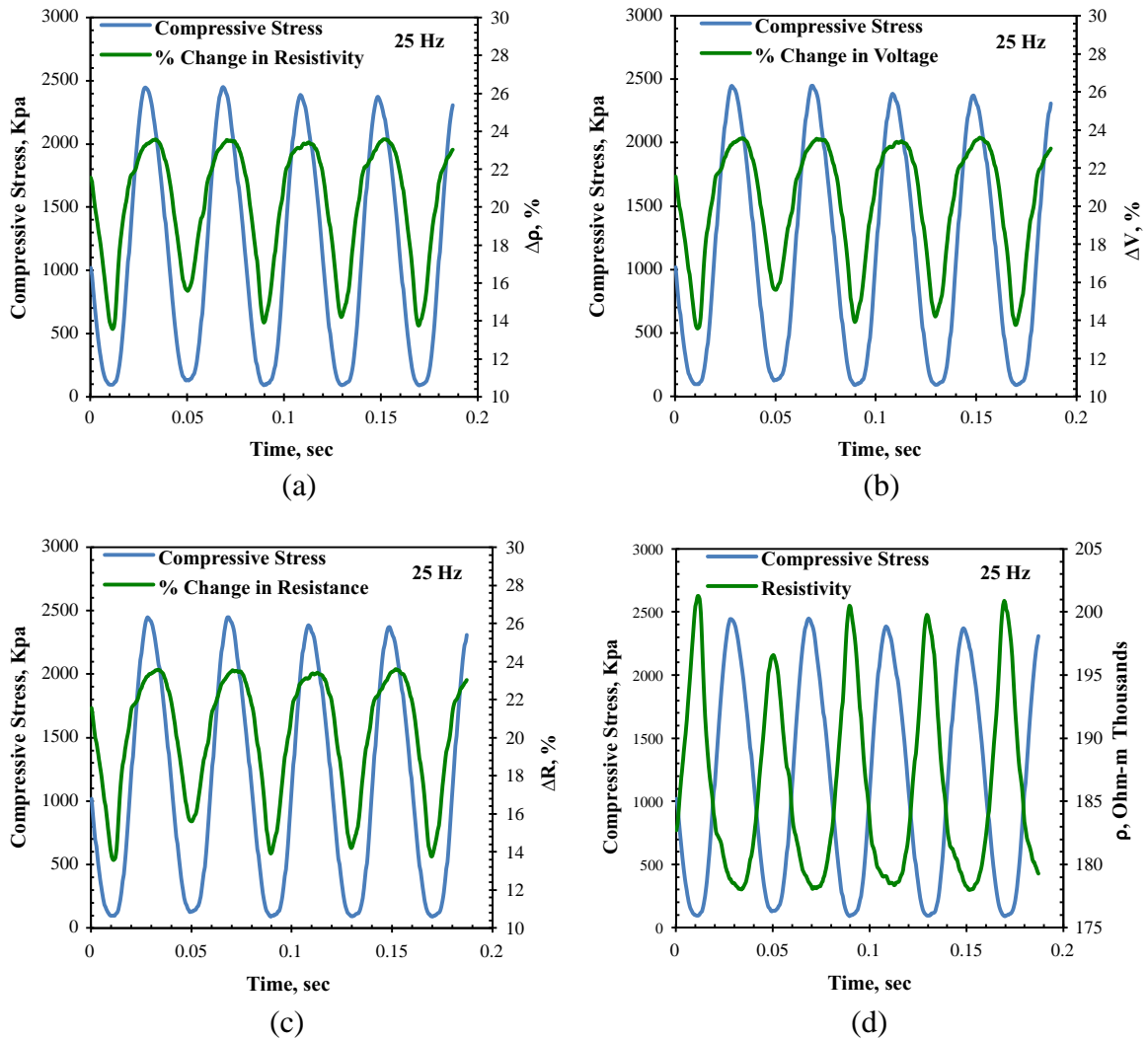


Fig. 2. (a) %Change in resistivity ($\Delta\rho$), (b) %change in resistance (ΔR), (c) %change in voltage (ΔV), and (d) resistivity (ρ), as a function of time and compressive stress.

electrodes and aggregates would be formed which will reduce the conductivity. Conductive silver paste was also used inside the holes to offer better contact between electrodes and conductive HMA however its loose contact was not successful for response measurements. Moreover, such samples were severely damaged and some others were broken during drilling process. It was also noticed that samples were affected with a potential cracking zone which could affect the mechanistic properties of the mixture. Electrodes were also tried to be embedded just after compaction in

order to take advantage of soft mixture. This method was not efficient because the sample was always fragile at that stage and embedding exercise on the sample at that stage caused de-shaping of sample, excessive damage and loose contact of the electrodes.

Finally, copper wires and copper plates were selected to be embedded in the sample during compaction process (Fig. 4). As discussed earlier in mixture design that the samples were compacted in 5 successive layers. Each layer was compacted to 5

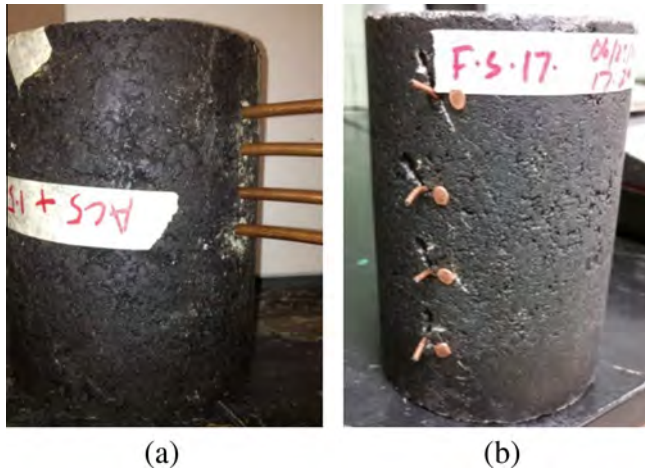


Fig. 3. Samples with (a) drilling and (b) hammering embedment of electrode.

gyrations. After every layer the copper wire was embedded. Fig. 4 shows the schematic and copper electrodes embedded in sample.

The surface area of the wire (2 mm dia) is very low as compare to the cross-sectional area of the sample (see Fig. 5) which facilitated in reduction of electrical signal disturbance while measuring the response of the mixture under cyclic loading. Furthermore, wire did not undergo excessive bending as compare to plates. It was observed that the wire seems to be fairly straight when embedded wired-sample was heated and split as shown in Fig. 5.

2.3.3. Uniaxial compression load testing

Following experiments were conducted to understand the piezoresistive response of CNF modified HMA mixtures.

1. *Frequency sweep test*-HMA specimens with embedded electrodes were subjected to dynamic frequency sweep test under compression loading. Testing was performed using a closed-loop servo-hydraulic machine, manufactured by Material Testing System (MTS). The mixtures were tested at frequencies of 25, 10, 5, and 1 Hz under stress control mode at 20 °C. Compression loading was applied, and the deformation was measured by using four surface mounted miniatures linear variable differential transformers (LVDT) in vertical directions and 90° apart. The gauge length for LVDT was kept at 57.2 mm.
2. *Repeated creep test*-Repeated compression creep loading test was conducted at 20 °C by applying a sustained compressive loading for 150 s and unloading of 150 s. The load, deformation and piezoelectric response were measured as stated above.

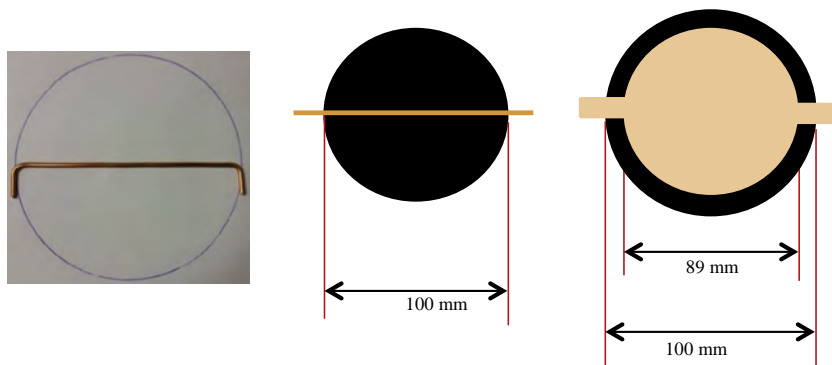


Fig. 4. Actual copper wire and schematic of wire and plate electrodes embedment in sample.

3. *Ramp loading*-Continuous compressive ramp loading was applied at a rate of 0.51 mm/min at room temperature. The test was stopped after a complete failure of the sample occurred. The deformations were measured and recorded as above.
4. *Repeated load permanent deformation (RLPD)*-Continuous haversine loading was applied with 0.1 s loading and 0.5 s rest period. The test was performed within the viscoelastic range of the mixture i.e. 80–100 microns. The test was conducted using the controlled temperature chamber at test temperatures of 20, 40 and 60 °C.

3. Results and discussion

3.1. Comparison of plate and wire electrodes

Fig. 6(a and b), shows the voltage signal obtained from loaded samples having different electrode types i.e. copper wire and copper plate. It can be observed that the voltage signal due to load is significantly higher in magnitude and smooth for the samples having wires as compare to the ones embedded with plate electrodes. Wire electrode sample showed consistent response of approximately 0.4 volts. On the other hand, the plate electrode sample showed approximately 0.02 volts. It should also be observed that noise-to-signal ratio of plate electrode is significantly higher than the wire electrode samples. Fig. 6(c and d), illustrates the signal of plate electrode and wire electrode samples, respectively. It can be observed that noise-to-signal ratio in plate electrode sample shown in Fig. 6(c) is significantly higher than the wire electrode samples as in Fig. 6(d). The possible reason of this is variation of electrical current flow in plate samples. Plates do not allow aggregates to pass through during compaction which results in de-shaping and amplified stress in certain zones of the plate. These amplified stress zones let excessive flow of current through that zone. This phenomenon creates an imbalance in the flow of current within the surface area of the electrode. Therefore, voltage signal which is directly recorded using automatic data collection during loading, showed disturbed signal. On the other hand wire electrode sample showed smooth and clean voltage signal. These stress zone phenomenon does not constitute in the wire electrode samples which results in smooth signals. Therefore, wire electrode samples were used throughout the study.

3.2. Comparison of binder types under ramp loading

Fig. 7 shows the stress and fractional change in resistance as a function of time of two types of conductive HMA constructed using PAC30 and AC5 with 6.5% LHT CNF at 20 °C. Strength test was conducted at a rate of 51 mm/min and signal was recorded during the



Fig. 5. Copper wire electrode in a sample after testing.

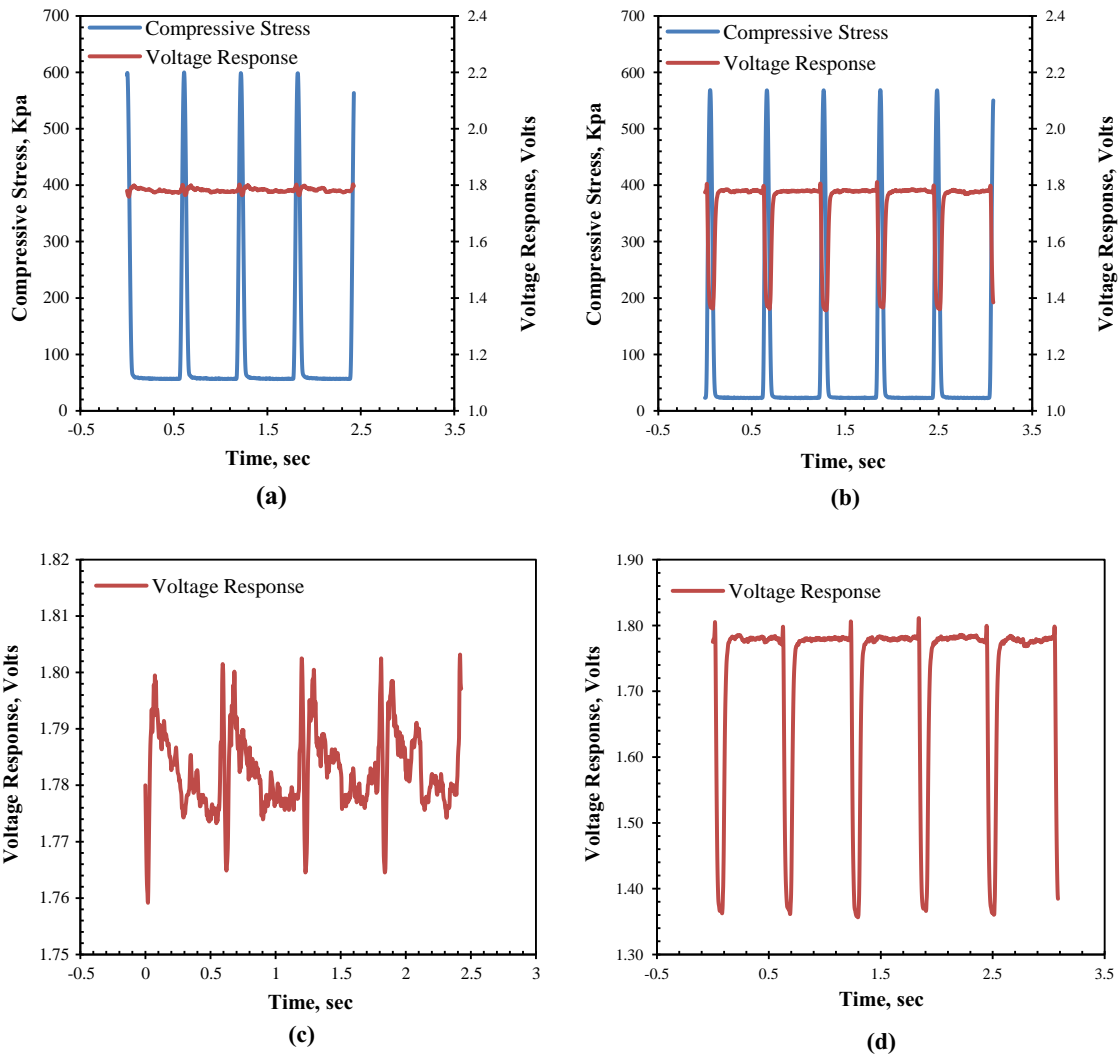


Fig. 6. Comparison of (a) plate and (b) wire electrodes, (c) signal of plate electrode sample (d) signal of wire electrode sample.

duration of test. It was desired to examine the behavior of percentage change in resistance of different conductive HMA samples experiencing in relation to damage and crack formation due to applied stress. The data in Fig. 7 can be divided in four zones: Zone-I: initial increase in $\Delta R/R$, Zone-II: decrease in $\Delta R/R$, Zone-III: secondary increase in $\Delta R/R$, and Zone-IV: final decrease in $\Delta R/R$. In order to explain the aforementioned zones, three types of phenomena should be considered (1) proximity effect (2) nano

and micro crack generation (3) dislocation of conductive path due to s movement of aggregates.

It can be observed that in the Zone-I $\Delta R/R$ follows stress increase, which is due to proximity effect. Zone-II exhibits decrease in $\Delta R/R$, which is due to micro/macro crack generation with stress increase. It was observed that both samples showed this behavior at about strain level of 3100 microns. This effect is due to micro/macro-cracks, which are playing their role in decreasing the

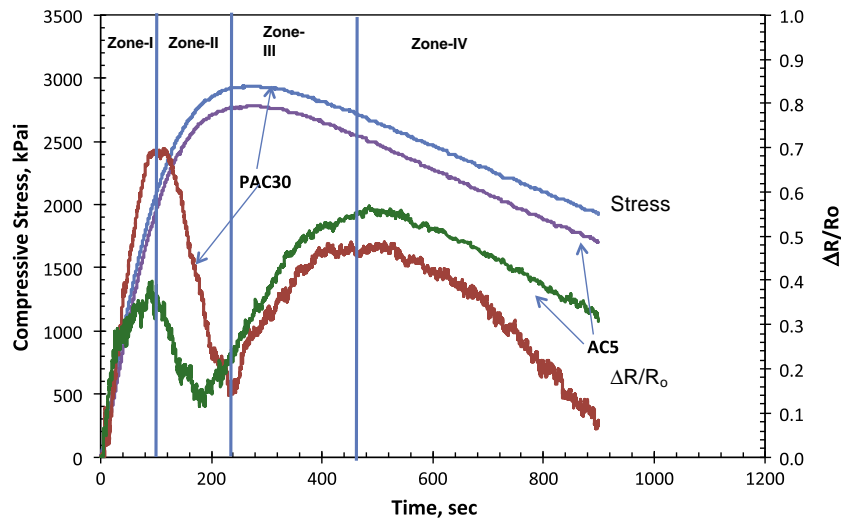


Fig. 7. Typical compressive stress and change in resistance as a function of time for CNF (LHT)-modified PAC30 and AC5 HMA under ramp loading.

change in resistance due to loss of conductive network. It is also important to note that proximity effect is underplaying in this zone. However, around the maximum strength level the proximity effect overcomes the micro/macro-crack effect and $\Delta R/R$ starts increase again as in Zone-III. The dislocation of conductive path due to high shear movement of the aggregates also played its role in Zone-II which incremented the effect of cracks. However, the sample started to bulge rapidly, which augmented the proximity effect in Zone-III and it carried on till the occurrence of fully developed macro cracks at final failure and breakage. At this stage the conducted path started to break vigorously and sample entered in Zone-IV in which the sample experienced a constant decrease in $\Delta R/R$.

The data in Fig. 7 also indicates that CNF modified PAC30 experienced more change in resistance as compare to CNF modified AC5 HMA. This difference is due to conductivity of the sample. CNF modified PAC30 is more conductive than the CNF modified AC5 sample. Higher conductive mixture exhibits higher response to loading. PAC 30 sample also exhibited smoother response as compare to AC5 sample. This is due to the stiffer nature of the PAC30 mixture. It is believed that the dislocation effect in conductive paths is less in PAC30 as compare to AC5 modified with CNF.

3.3. Piezoresistive response under sinusoidal loading

Fig. 8 depicts the resistivity response of HMA mixtures modified with two different types of CNF at 25 Hz and 10 Hz at 20 °C. Fig. 8(a and b) shows the response of 5.3% CNF-LHT modified HMA whereas Fig. 8(c and d) illustrates the response of 8.5% CNF-XTPS modified HMA. The differences in CNF dosages were due to less conductive characteristics of CNF-XTPS. CNF-LHT is more conductive than CNF-XTPS therefore it was desired to increase the percentage of CNF-XTPS in binder to get reasonable response from the sample due to load. The least CNF dosage at which sample started to produce a reasonable response under loading was found to be 8.5% and 5.3% for CNF-XTPS and CNF-LHT modified HMA mixtures, respectively.

The initial resistivity measurements of CNF-XTPS and CNF-LHT modified mixture were found to be 131.5 k Ω -m and 165.7 k Ω -m, respectively. The resistivity of LHT is more than XTPS. The possible reason is the CNF dosage introduced in XTPS. The percentage of fiber in XTPS is 50% more than the LHT. The average response of

LHT and XTPS samples at 25 Hz is 22 k Ω -m and 11 k Ω -m, respectively. On the average the difference in maximum and minimum value of percentage responses of CNF-LHT and CNF-XTPS modified mixtures are 14% and 8%, respectively. This indicates that CNF-LHT has better response abilities under cyclic loading as compare to CNF-XTPS. Furthermore, the signal is very clear for CNF-LHT and only few abruptions can be noticed especially, when the stress is its highest level. The reason of this variation in signal is due to the transitional stage, where proximity effect and dislocation of conductive paths and micro-cracks become functional. This transition is simultaneously overcome by proximity effect as soon as the sample starts recovery and cracks are healed and dislocation is restored. It can also be observed in Fig. 8(b) that there is an overall decreasing trend of percent change in resistivity ($\% \Delta \rho$) at 10 Hz for CNF-LHT modified mixtures. However, this trend was not significant for CNF-XTPS modified mixtures as shown in Fig. 8(d). The possible reason is an overall increasing plastic strain in the CNF-LHT mixtures. In order to evaluate and explore this phenomenon percent change in resistivity ($\% \Delta \rho$) was plotted at 1 Hz for both types of CNFs (Fig. 9).

Fig. 9 illustrates the results of both CNF-LHT and CNF-XTPS modified mixtures at 1 Hz and 20 °C. The percent change in resistivity ($\% \Delta \rho$) is plotted with compressive strain to understand the overall decreasing $\% \Delta \rho$ trend. Fig. 9 shows that mixtures are still responding well at 1 Hz; however overall decreasing trends in percent change in resistivity, which could not be observed at higher frequencies such as 25 Hz was observed. This trend is unique as this overall decrease of percent change in resistivity will eventually affect the piezoresistive response of the mixtures at higher number of load cycles. HMA mixtures show viscous behavior at higher temperature or low frequencies. At 1 Hz the behavior of the mixture is relatively viscous and it accumulates more plastic strain. It is interesting to note that although plastic strain enhances the proximity effect which means that overall resistivity should decrease however, the percent change in resistivity decreased indicating an increase in initial resistivity (ρ_0). In the beginning percent change in resistivity increased; however after third cycles it started to decrease. This could be due to excessive plastic strain accumulated in the sample. This graph showed that the permanent strain was accumulated at this stage. The initial trend of decreasing resistivity could be explained with proximity effect, whereas after third cycle it seemed that dislocation of conductive path and crack growth caused the overall

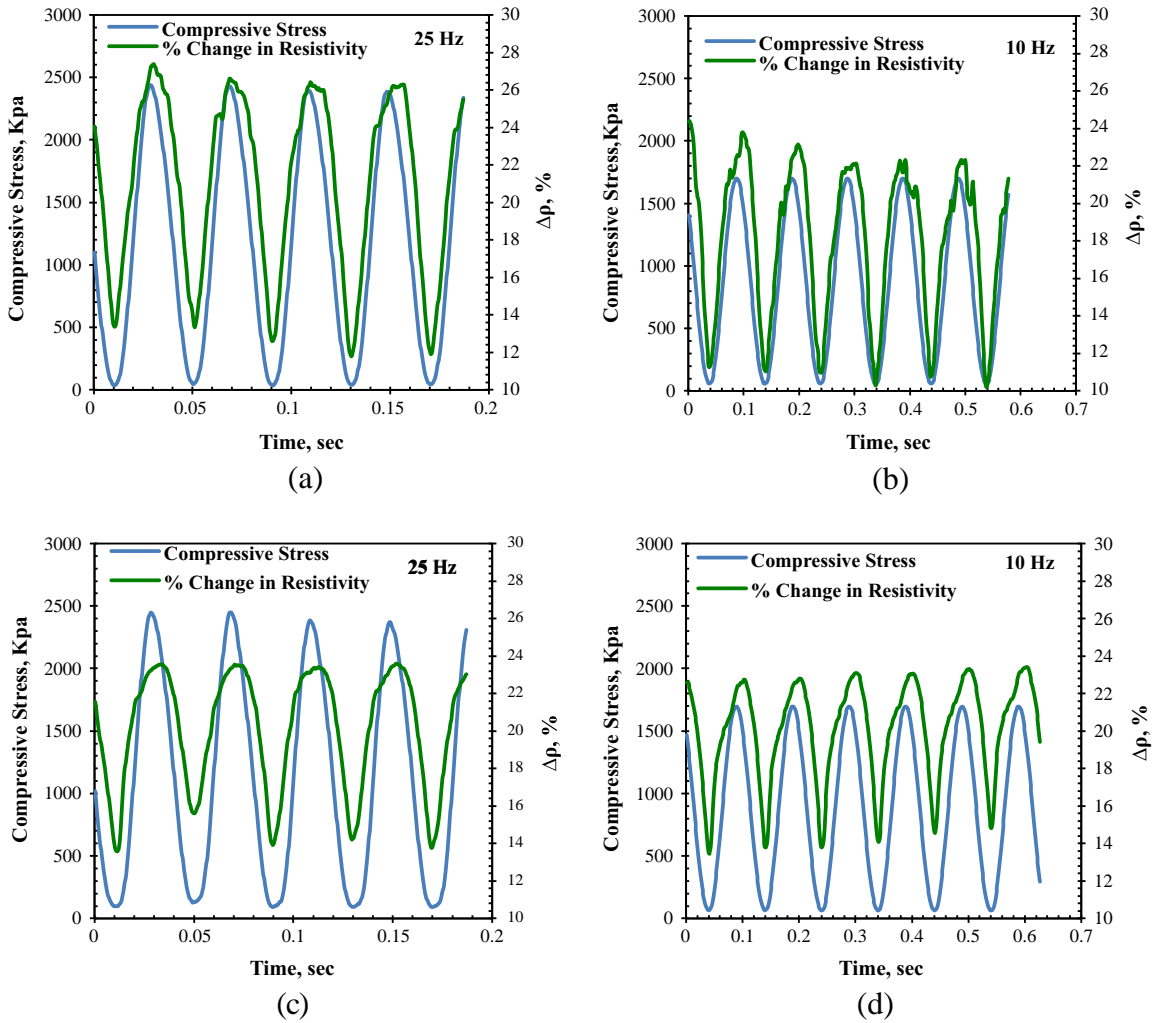


Fig. 8. 5.3% CNF-LHT PAC-30 resistivity response at (a) 25 Hz and (b) 10 Hz, 8.5% CNF-XTPS PAC-30 resistivity response at (c) 25 Hz and (d) 10 Hz.

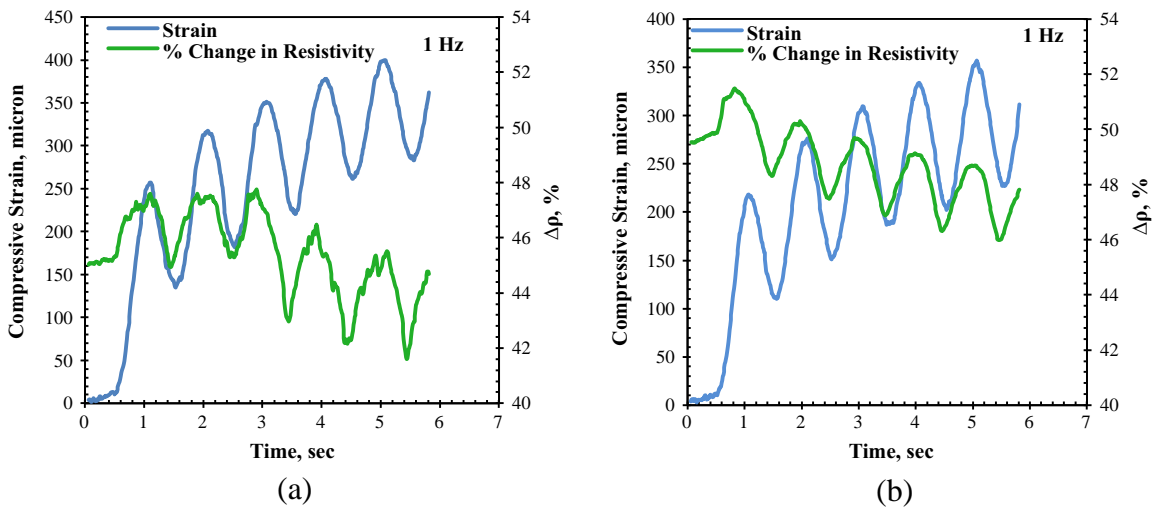


Fig. 9. (a) 5.3% CNF-LHT PAC30 resistivity response with compressive strain at 1 Hz. (b) 8.5% CNF-XTPS PAC30 resistivity response with compressive strain at 1 Hz.

resistivity of the sample to increase. This mechanism inevitably decreased the percent change in resistivity of the samples. Somewhat similar trend was observed in the CNF XTPS modified HMA mixtures. However, the initial decreasing trend was not significant in that sample.

3.4. Piezoresistive response under repeated creep loading

Fig. 10(a) shows the effect of repeated creep square loading on percentage response of resistivity of the conductive HMA mixtures modified with CNF-LHT. It can be observed that percent change in

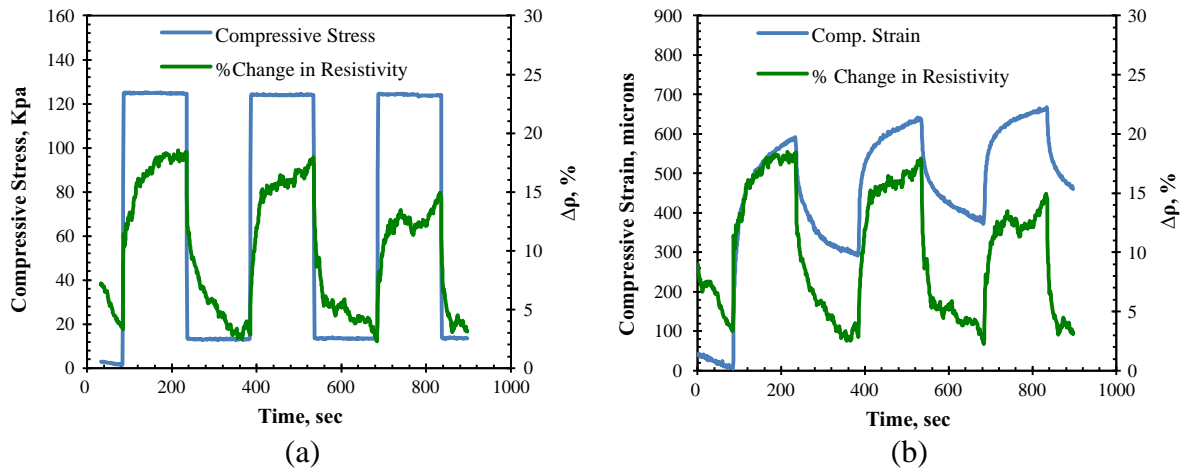


Fig. 10. Piezoresistive response of 5.3% CNF-LHT PAC30 HMA mixture under repeated creep loading, (a) compressive stress, and (b) compressive strain.

resistivity ($\% \Delta \rho$) follows the compressive stress in resilient manner up to maximum stress level; however percent change in resistivity keeps on increasing under sustained stress. It resiliently follows the stress release and keeps on decreasing while the mixture is at rest. This trend is because of viscoelastic behavior of HMA mixtures. The time dependent strain and strain recovery functionalizes proximity effect and resistivity follows this pattern. Fig. 10(b) shows the comparison of percent change in resistivity and compressive strain under square loading. It is obvious from Fig. 10(b) that change in resistivity is following the viscoelastic behavior of the conductive HMA. The resistivity decreases with increase in strain and keeps on decreasing with time dependent effect of strain, which functionalizes the proximity effect and this behavior increases percent change in resistivity response. Overall plastic strain accumulation can also be observed in the Fig. 10(b) and percent change in resistivity is also exhibiting decreasing trend, which is similar to the results reported in Fig. 9. The resistivity is related to plastic strain in reverse manner. This relation is believed to be due to dislocation of conductive path and crack generation in the mixture. This result further approves the similar trends shown under sinusoidal loading. Interesting thing to notice is that the response behavior is resilience. Resistivity response follows strain's elastic response during loading i.e. the response of the sample is instantaneous when load is applied on the sample. This is promising result in relation to the piezoresistive response of HMA mixture.

Fig. 11 exhibits the piezoresistive response of 8.5% CNF-XTPS PAC30 conductive HMA mixture under repeated creep loading using square loading. The percent change in resistivity follows compressive stress similarly as was observed in CNF-LHT modified mixtures (see, Fig. 10). Overall decrease in percent change in resistivity can be observed due to creep effect. The creep causes damage and crack initiation which results in dislocation of conductive path. After a longer period of time this effect becomes prominent and resistivity of the mixture increases. Fig. 11(b) depicts piezoresistive response with compressive strain in repeated creep loading. An important observation in this plot is the non-viscoelastic response of change in resistivity of the conductive HMA especially in first two cycles. This response is due to the high stiffness of the material which resists the crack mechanism. The lower crack generation in the stiffer material keeps the proximity effect more effective than the crack and dislocation mechanisms. The percent change in resistivity shows consistency during the rest period. However, this resistance mitigates and the effect of cracks and dislocation seems to overcome proximity effect and viscoelastic behavior of percent change in resistivity is observed again in last two cycles. Overall,

similar response of percent change in resistivity can be observed in this mixture as compare to CNF-LHT modified sample, yet with a change in signal strength, which is due to the stiffness of the material.

It should also be observed that the percentage responses of CNF-LHT and CNF-XTPS modified HMA mixtures under repeated creep loading are 15% and 5%, respectively. Recall that the respective responses of CNF-LHT and CNF-XTPS under sinusoidal loading were 14% and 8%. This shows that CNF-LHT maintains its response strength even under different set of loading.

3.5. Piezoresistive response at different temperatures

Since 5.3% CNF-LHT modified HMA mixtures exhibited strong and better piezoresistive response such mixtures were selected to evaluate the effect of temperature. Haversine wave form of 0.1 s loading and 0.5 s of rest period was used and change in resistivity with the change in stress and strain were monitored at temperatures of 20 °C, 40 °C and 60 °C Fig. 12(a and b) depicts the piezoresistive response of CNF-LHT HMA mixtures under haversine loading at 20 °C. The data in the figure reveals that the response is fairly clean and smooth. HMA mixture responded to the loading in a precise manner. It can be observed that overall percent change in resistivity does not show increasing or decreasing trend within the five loading cycles. Possible reason for this was low rate of accumulation of plastic strain at room temperature. It was observed that the voltage response lagged the strain response of HMA by 8–12°. Fig. 13(a and b) depicts the piezoresistive response in terms of percent change in resistivity with compressive stress at 40 °C and 60 °C, respectively. It can be seen that percent change in resistivity exhibited resilient decrease at the time when stress was applied, which was not normal behavior, as the response should increase on application of stress; however it followed the expected trend of increase afterwards. Possible explanation of this effect was disconnection between material and electrode. When load was applied the conductive material holding the wires underwent deformation and temporarily disconnects from the wire due to shear forces applied on the material around the wire, this dislocation decreased the response. However this connection was reestablished quickly because of the compressive stress which pushed the material down to reconnect the wire. Another possible reason of this response could be the rate of loading. A sudden impact of load just after the rest period might cause dislocation and temporary disconnection of the material and electrode contacts for a fraction of second. This behavior was not found in sinusoidal loading as the loading wave was continuous and there was no rest period. How-

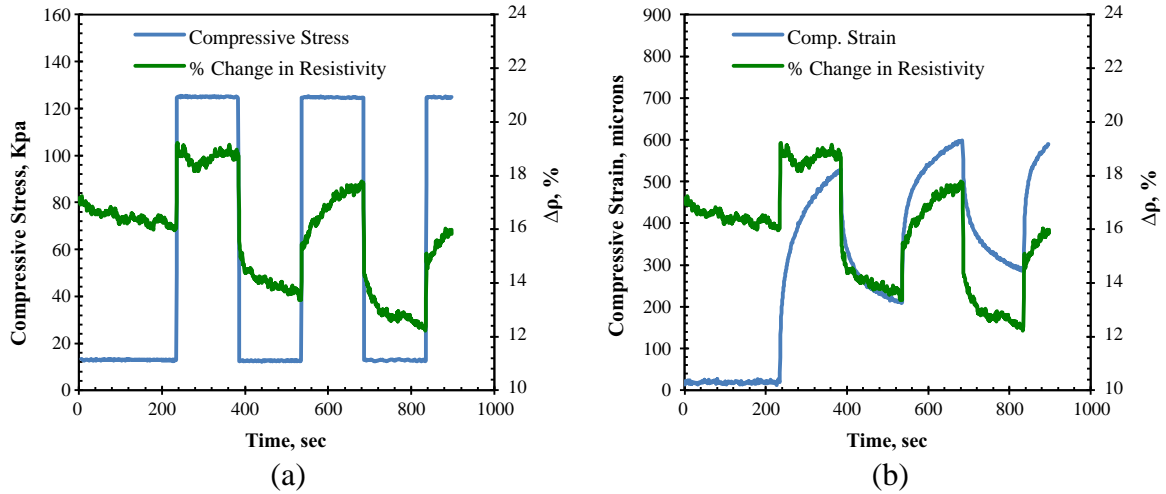


Fig. 11. Piezoresistive response of 8.5% CNF-XTPS PAC30 sample under repeated creep loading, (a) compressive stress with $\Delta\rho$, and (b) compressive strain with $\Delta\rho$.

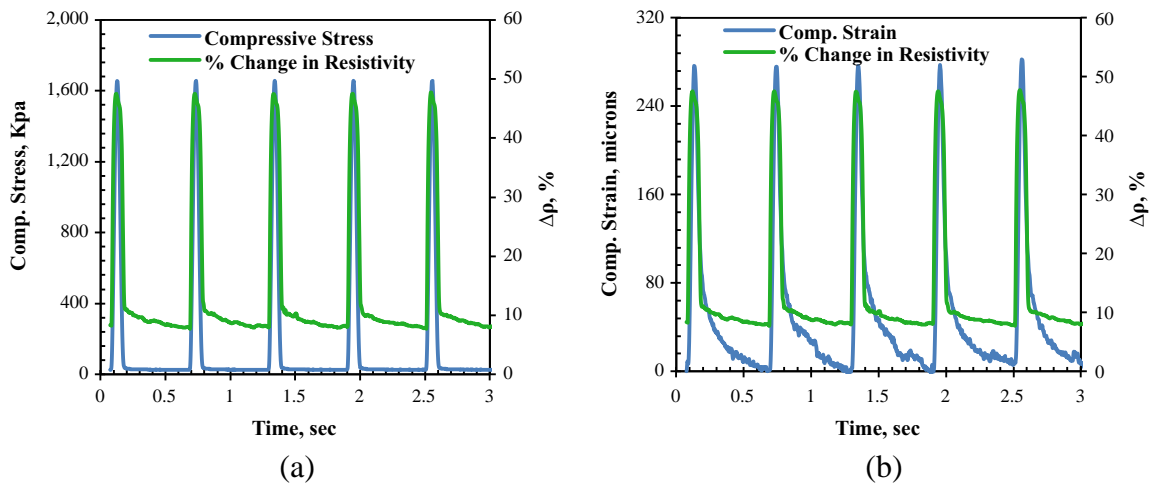


Fig. 12. (a) Piezoresistive response of 5.3% CNF-LHT PAC30 mixture under haversine loading with compressive stress 20 °C (b) with compressive strain at 20 °C.

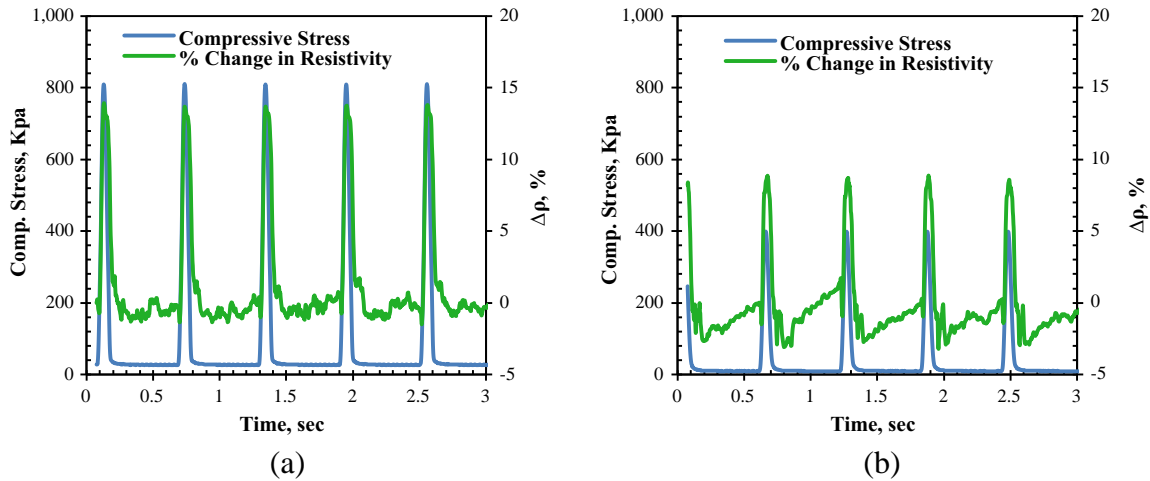


Fig. 13. Piezoresistive response of 5.3% CNF-LHT PAC30 mixture under haversine loading with compressive stress (a) 40 °C (b) 60 °C.

ever, the repeated creep loading exhibited similar trend, but it was negligible.

Response of the mixture at 40 °C is similar to the response at 20 °C and no abnormality in the response could be observed.

However, response at 60 °C showed increasing trend during rest period. If response is observed closely, it can be seen that the response bounced back to same level where it started reacting on loading. When load was removed the response decreased in

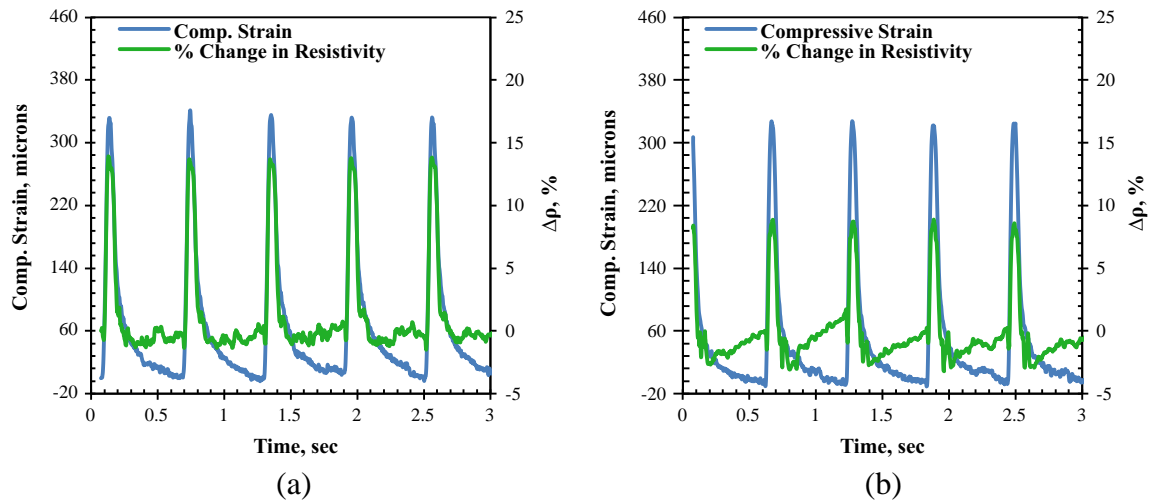


Fig. 14. Piezoresistive response of 5.3% CNF-LHT PAC30 mixture under haversine loading with compressive strain (a) 40 °C (b) 60 °C.

resilience however it crossed a certain level in each cycle and then it came back down at the level where it started to react on loading. This behavior might be due to high temperature. HMA mixture is softer at 60 °C as compare to lower temperatures and when load was suddenly removed material showed elastic recovery quickly and response followed this sudden recovery. After elastic recovery the viscoelastic strain started to recover thereby establishing new electric contacts through micro crack healing.

The aforementioned phenomenon could be explained through the difference between structured and free binder in the conductive HMA mixtures. It is important to note that conductive HMA under consideration has two phases of application of conductive fillers: (1) CNF in binder and (2) CNF in aggregates. The thin film coating of aggregate is called structured binder, whereas rest of the binder is called free binder. When loading is applied to the sample the resistivity of conductive HMA decreases and vice versa. This decrease is believed to be due to proximity effect. However, during rest period the temperature plays its role and binder continues to expand, which inevitably functionalize the free binder to generate some more contacts within the mix and keep increasing the response. Viscoelastic strain continues to decrease having a diminishing effect. This recovery of strain has lesser role to play in this mechanism. However, the sample not only subjected under compressive strains, yet it experiences tensile strain. The effect of compressive strain is more prominent during loading cycle, yet the role of tensile strain recovery cannot be neglected during rest period, especially at high temperature. This tensile strain recovery brings the CNF closer to each other and thermal expansion phenomenon of free conductive binder also provides connection for the flow of electricity. This composite effect results in decrease in resistivity during rest period of viscoelastic strain recovery. It can also be observed in Fig. 13(a and b) that percent change in resistivity of the sample at 40 °C is approximately 15% whereas at 60 °C the percent change in resistivity reduces to 9%. However, it should also be observed that the applied stress is 800 psi and 400 psi at 40 °C and 60 °C, respectively. It is believed that piezoresistive response is mainly a function of elastic strain, therefore stress levels were altered to maintain the elastic strain level of 300 ± 20 microns (Fig. 14). It can be observed that the piezoresistive response decreased significantly. This decrease in response is believed to be due to temperature effect. The possible reason is due to high temperatures the material gets softer and for the same compressive strain it experiences more lateral strain relative to the low temperatures. Due to this high lateral strain the CNF network is disturbed resulting in lower piezoresistive response.

Fig. 14(a and b) shows the response of the material at 40 °C and 60 °C with compressive strain. It can be observed that at 40 °C (Fig. 14(a)) strain behaves in viscoelastic manner at rest period however resistivity remains constant, whereas at 60 °C it decreases during viscoelastic period. The consistency of resistivity at 40 °C might be due to stiffness of material. As there is negligible plastic strain accumulation in the sample during the cycle therefore resistivity remains constant. The proximity effect does not come into play due to negligible amount of strain and high resistivity.

In short, overall response of conductive-HMA at 40 °C and 60 °C is phenomenal. It is following the loading cycles successively and without any abnormality and noise. This is promising result for future studies. This also proves that CNF-LHT transformed HMA into an effective piezoresistive material which responds at different frequencies, loading type and at different temperatures.

3.6. Phase angle between material and piezoresistive responses

Phase angles between the strain and voltage responses were determined for both sine wave and haversine wave forms of loading and are reported in Table 2. It must be noted that due to heterogeneous nature of HMA mixture some variation were observed in phase angle calculation. Occasionally the voltage signals exhibited uneven behavior at the peak load. Therefore, best fit curves were utilized to obtain the maximum strain and voltage responses along with the times to reach to the maximum values for various types of loadings. The data in the table illustrates that the voltage response lagged the strain response of CNF HMA mixtures. Under sinusoidal wave form there existed some frequency dependency in phase angles. The average phase angle at 20 °C slightly increased at 25–10 Hz and then decreased at 5 Hz, however, the difference in phase angle values were not statistically significant at α value of 0.05. On the other hand, the sufficient temperature dependency could be

Table 2
Summary of phase angle (degree) between strain and voltage responses.

| Loading type | Temperature, °C | Frequency, Hz | | |
|-----------------|-----------------|---------------|------------|------------|
| | | 25 | 10 | 5 |
| Sinusoidal wave | 20 | 10.5 (1.5) | 14.1 (2.2) | 12.6 (2.7) |
| Haversine wave | 20 | – | 11.7 (3.8) | – |
| | 40 | – | 29.4 (4.8) | – |
| | 60 | – | 41.2 (3.5) | – |

Number in parenthesis “()” indicates standard deviation values.

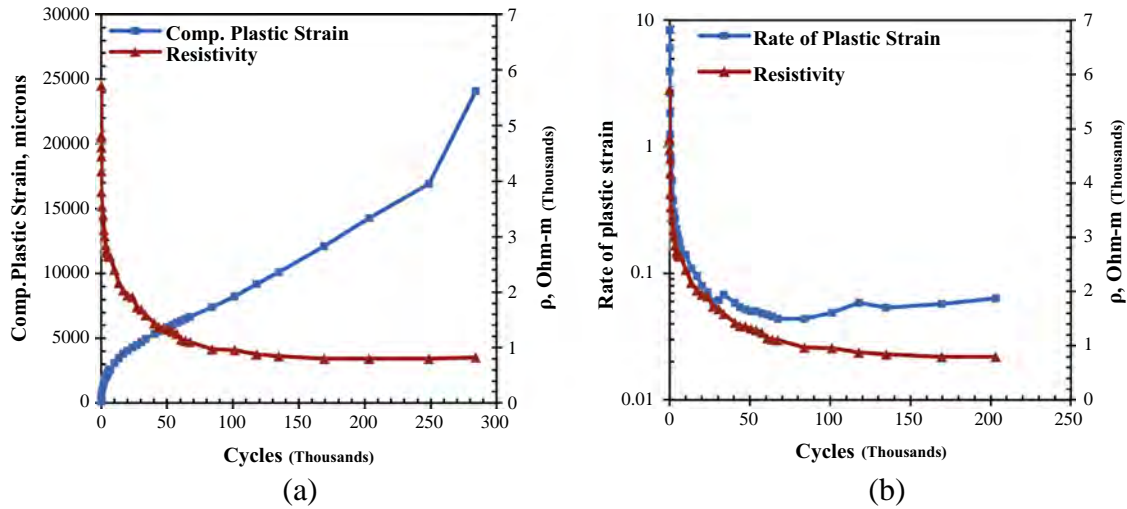


Fig. 15. Resistivity behavior of 5.3% CNF-LHT PAC30 under constant haversine stress with number of cycles and compressive plastic strain RLPD at 20 °C (a) plastic strain and resistivity (b) rate of plastic strain and resistivity.

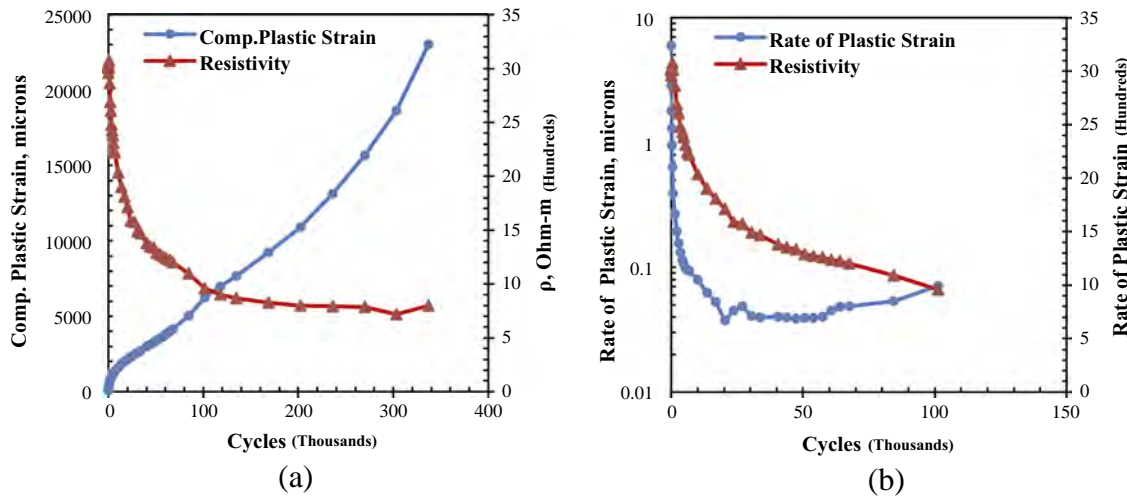


Fig. 16. Resistivity behavior of 5.3% CNF-LHT PAC30 under constant haversine stress with number of cycles and compressive plastic strain RLPD at 40 °C (a) plastic strain and resistivity (b) rate of plastic strain and resistivity.

observed for haversine loading wave form of 10 Hz as shown in Table 2. The phase angle increased with the increase in temperature. The coefficient of variation ranged from about 8–32%. The variation was high at low temperature as compared to high temperatures. It was found that phase angle between strain and voltage responses were statistically significantly different at different temperatures at α value of 0.05.

3.7. Resistivity behavior under repeated haversine loading (RLPD)

Figs. 15–17 illustrate the resistivity (ρ) behavior of the conductive HMA modified with 5.3% CNF-LHT under repeated loading at 20 °C, 40 °C and 60 °C, respectively. All samples exhibited similar trend at all temperatures which is very promising. When resistivity is plotted with accumulated compressive plastic strain it shows that resistivity is inversely proportional to accumulated plastic strain. Therefore the resistivity was also plotted with rate of change of cumulative compressive plastic strain for each temperature. In initial cycles the rate of strain is high which mitigates in middle period and then it starts increasing again in third period

where sample starts macro-cracking. The slope of resistivity curve shows that it follows this behavior in conformity. First period where strain rate is higher proximity effect is playing its role in decreasing the resistivity. The electrodes come closer and more contacts are developed within the sample, which eventually decrease the resistivity. However, micro-cracks are generated in second zone where strain accumulation rate drops. These cracks initiate the dislocation of conductive path and cracks generation phenomena in the sample. Proximity effect gradually reduces and dislocation and crack phenomena gradually over comes the proximity effect. Dislocation and crack generation are detrimental for conductivity of any material. Therefore, rate of decrease in resistivity also mitigates and sample come into an equilibrium state. This equilibrium state carries on until an increasing trend due to macro-cracking zone is observed which overcomes proximity effect. This result shows that the behavior of resistivity is not affected by temperature. Resistivity of the sample decreases with increase in plastic strain and then it stabilizes for a longer period of time, as number of cycles increase and sample experiences macro-crack generation the resistivity also starts to increase.

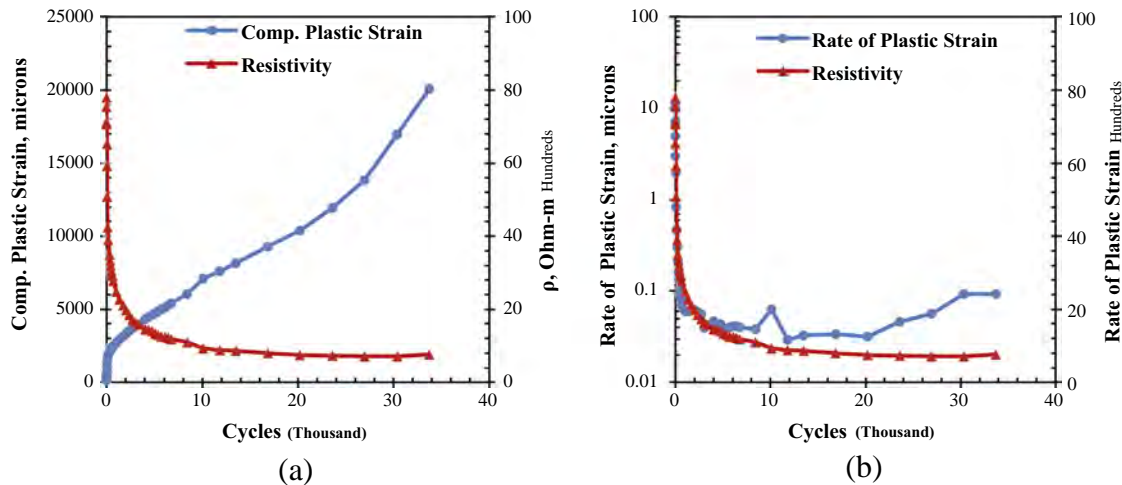


Fig. 17. Resistivity behavior of 5.3% CNF-LHT PAC30 under constant haversine stress with number of cycles and compressive plastic strain RLPD at 60 °C (a) plastic strain and resistivity (b) rate of plastic strain and resistivity.

4. Conclusions and recommendations

In this study an exploratory investigation of piezoresistive response of CNF modified HMA mixtures under various types of loading at different load frequency and temperature was conducted. Stress–strain response due to applied load and its relationship with the change in resistivity was studied. Based on the experimentation and analyses of test results following conclusions and recommendations were drawn:

- Dry mixing process provides reliable and consistent results in piezoresistive response study. However, the wet process is time consuming and environmentally hazardous. Therefore, it is recommended that the dry mixing process be used in future studies.
- Wire embedded electrode provide smoother and better results in comparison to plate electrodes. Moreover, wire electrodes are easier to install, economical and time conserving method of electrode embedment. It is recommended that the electrodes should be embedded during compaction as after compaction it is not only cumbersome but destructive for the mixtures.
- Modified PAC30 and AC5 exhibited similar results in piezoresistive response. However, modified PAC30 showed higher response, smoother and cleaner signals as compared to modified AC5 mixture. Moreover, modified PAC30 is stronger in mechanistic properties of the binder; therefore it is recommended to use such mixtures for further research.
- Both type of CNF (LHT and XTPS) used in the study showed positive piezoresistive response; however, CNF-LHT exhibited better results in terms of significant response as compared to the CNF-XTPS. CNF-LHT dosage was also less relative to CNF-XTPS, which proves it to be economical as well. Therefore, CNF-LHT is recommended for similar testing in future.
- CNF-LHT exhibited promising piezoresistive response at different loading types and loading frequencies. This indicates that CNF-LHT is suitable conductive material to transform HMA into a piezoresistive material. This indicates that material senses the load at different levels of frequencies and temperatures. Further, it provide encouraging basis to use this material as sensors for further applications.
- Temperature slightly affect the response of the CNF modified HMA mixtures. However, sufficient change in resistivity with the change in load was observed at 20 °C, 40 °C and 60 °C. The modified mixture holds a promise in sensing traffic loads at various temperatures.

- It was found that the voltage response lagged the strain response and was mainly a function of temperature. The phase angle increased with the increase in temperature. It is recommended to conduct detailed investigate of the phase angle between strain and electrical parameters at different temperatures, stress levels and loading frequencies.
- Repeated loading cycles decreased the overall resistivity of the mixtures at all temperatures. The decrease in resistivity values was directly proportional to the rate of accumulation of plastic strain. This is an interesting finding that needs further investigation as the response is also affected by the resistivity value at a given loading cycle.

Acknowledgments

The authors wish to express their sincere thanks to the University of Louisiana at Lafayette and the Louisiana Transportation Research Center-Transportation Innovation for Research Exploration (TIRE) program for their financial support. Special thanks are extended to Mr. Mark for assisting in experimentations.

References

- [1] S. Abtahi, R. Khodadadi, S.M.T.E. Hejazi, A feasibility study on the use of propylene fibers as a modifier in asphalt-concretes made from steel slag, in: 4th International Conference on Bitumen & Asphalt, Tehran, Iran, 2008.
- [2] L.D. Minsk, Electrically conductive asphalt for control of snow and ice accumulation, Highway Res. Rec. 227 (1968) 57–63.
- [3] S.P. Wu, L.T. Mo, Z.H. Shui, et al., An improvement in electrical properties of asphalt concrete, J. Wuhan Univ. Technol. (Mater. Sci. Ed.) 17 (4) (2002) 69–72.
- [4] P. Pan, W. Shaopeng, X. Feipeng, P. Ling, X. Yue, Conductive asphalt concrete: a review on structure design, performance, and practical applications, J. Intell. Mater. Syst. Struct. (2014).
- [5] M. Rosli, I. Nur, M.S. Fahimi, M. Abdulaziz, S.H. Anwar, F. Wasid, Steel slag as an aggregate replacement in Malaysian hot mix asphalt, ISRN Civ. Eng. 2012 (2012) 5.
- [6] L. Xiaoming, W. Shaopeng, Study on the graphite and carbon fiber modified asphalt concrete, Constr. Build. Mater. 2011 (4) (2010) 1807–1811.
- [7] L.e.a. Xiaoming, Properties evaluation of asphalt-based composites with graphite and mine powder, Constr. Build. Mater. 2008 (22) (2008) 121–126.
- [8] Y. Qun, L. Xu, W. Ping, z. Hong-Wei, Electrical signal characteristics of conductive asphalt concrete in the process of fatigue cracking, Smart Struct. Syst. 14 (3) (2014) 469–477.
- [9] N. Tang, S.P. Wu, M.Y. Chen, P. Pan, C.J. Sun, Effect mechanism of mixing on improving conductivity of asphalt solar collector, Int. J. Heat Mass Transfer 75 (2014) 650–655.
- [10] Y. Qun, L. Xu, W. Ping, Resistivity measurement of conductive asphalt concrete based on two-electrode method, J. Central South Univ. 20 (9) (2013) 2599–2604.

- [11] W. Shaopeng, P. Pan, C. Mingyu, Z. Yuang, Analysis of characteristics of electrically conductive asphalt concrete prepared by multiplex conductive materials, *J. Mater. Civ. Eng.* 25 (7) (2013) 871–879.
- [12] S. Aizawa, T. Kakizawa, M. Higashino, Case study of smart materials for civil structures, *Smart Mater. Struct.* 7 (5) (1998) 617–626.
- [13] D.L. Zhang, L. Zhongjin, K.-R. Wu, 2-2 piezoelectric cement matrix composite: Part II. Actuator effect, *Cem. Concr. Res.* 32 (5) (2002) 825–830.
- [14] R.F. Stratfull, Experimental cathodic protection of a bridge deck, *Transp. Res. Rec.* 500 (1974) 1.
- [15] P.L. Zaleski, D.J. Derwin, W.H. Flood, Electrically conductive paving mixture and paving system, United States Patent US Patent. 5, 707, 171, 1998.
- [16] W. Shaopang, L. Mo, Z. Shui, D. Xuan, W. Yang, Y. Xue, Preparation of electrically conductive asphalt, *J. Wuhan Univ. Technol. (Transp. Sci. Eng. Ed.)* 26 (2) (2002) 567.
- [17] H. Baoshan, C. Xingwei and S. Xiang, Effects of electrically conductive additives on laboratory-measured properties of asphalt mixtures, *Materials in Civil Engineering*, 2009.
- [18] F. Hussain, M. Hojjati, M. Okamoto, R. Gorga, Review article: polymer-matrix nanocomposites, processing, manufacturing, and application: an overview, *J. Compos. Mater.* 40 (17) (2006) 1511–1575.
- [19] W.-J. Lee, S.-E. Lee, C. Kim, The mechanical properties of MWNT/PMMA nanocomposites fabricated by modified injection molding, *Compos. Struct.* 76 (4) (2006) 406–410.
- [20] L. Xiaoming, W. Shaopeng, Research on the conductive asphalt concrete's piezoresistivity effect and its mechanism, *Constr. Build. Mater.* 23 (8) (2009) 2752–2756.
- [21] M. Xiao, W. Shaopeng, Study on piezoresistivity character of electrically conductive asphalt concrete, *Adv. Mater. Res.* 233–235 (May 2011) 1756–1761.
- [22] W. Shaopeng, L. Mo, Z. Shui, C. Z. Investigation of conductivity of asphalt concrete containing conductive fillers, *Carbon* (2005) 1343–1358.
- [23] D. Chung, Damage in cement-based materials, studied by electrical resistance measurement, *Mater. Sci. Eng.* 42 (2003) 1–40.
- [24] J.-C. Lin, L.C. Chang, H.L. Ho, Mechanical behavior of various nanoparticle filled composites at low-velocity impact, *Compos. Struct.* 74 (1) (2005) 30–36.
- [25] S. Kumar, T. Rath, R.N. Mahaling, C.K. Das, Processing and characterization of carbon nanofiber/syndiotactic polystyrene composites in the absence and presence of liquid crystalline polymer, *Compos. Part A: Appl. Sci. Manuf.* 38 (5) (2007) 1304–1317.
- [26] B.e.a. Fiedler, Fundamental aspects of nano-reinforced composites, *Compos. Sci. Technol.* 66 (16) (2006) 3115–3125.
- [27] M.J. Khattak, A. Khattab, H.R. Rizvi, Characterization of carbon nano-fiber modified hot mix asphalt mixtures, *Constr. Build. Mater.* 40 (2013) 738–745.
- [28] M.J. Khattak, A. Khattab, H.R. Rizvi, P. Zhang, The impact of carbon-nanofiber modification on asphalt binder rheology, *Constr. Build. Mater.* 12 (22) (2011) 257–264.
- [29] M.J. Khattak, A. Khattab, H.R. Rizvi, Mechanistic characteristics of asphalt binder and asphalt matrix modified with nano-fiber, *Proceedings of Geo-Frontiers 2011: Advances in Geotechnical Engineering Dallas*, 2011.
- [30] Hashim Reza Rizvi, Impact of carbon nanofibers on the mechanistic and piezoresistive characteristics of asphalt binders and hot mix asphalt mixtures (Master of Science Thesis), University of Louisiana at Lafayette, Summer 2012.